Appl. Math. J. Chinese Univ.
2026, 41(1): 181-193

On one dimensional advection-diffusion equation with variable diffusivity

Eeshwar Prasad Poudel[1,3] Pitambar Acharya[2]
Jeevan Kafle[3,*] Shreeram Khadka[3]

Abstract. In our study, we tackle a linear advection-diffusion equation that varies with time and is constrained to one dimension, under the framework of homogeneous Dirichlet boundary conditions. We employ two distinct approaches for solving this equation: an analytical solution through the method of separation of variables, and a numerical solution utilizing the finite difference method. The computational output includes three dimensional (3D) plots for solutions, focusing on pollutants such as Ammonia, Carbon monoxide, Carbon dioxide, and Sulphur dioxide. Concentrations, along with their respective diffusivities, are analyzed through 3D plots and actual calculations. To comprehend the diffusivity-concentration relationship for predicting pollutant movement in the air, the domain is divided into two halves. The study explores the behavior of pollutants with higher diffusivity entering regions with lower diffusivity, and vice versa, using 2D and 3D plots. This task is crucial for effective pollution control strategies, and safeguarding the environment and public health.

§1 Introduction

Advection is defined as a transmission of a matter from one place to another inside a moving fluid [19]. Diffusion can be described as the change of molecules from high concentration to low concentration because of the driving force [18]. The general scalar transport equations including the phenomenon advection and diffusion are broadly termed as advection-diffusion equation (ADE) [6]. In the natural environment, the movement of fluids occur through the combined influences of advection and diffusion [2]. ADEs are crucial in applied mathematics and extensively utilized for simulating various processes in environmental sciences, biological sciences, chemical engineering, and hydrology [16]. ADE in mathematical modelling also has

Received: 2024-01-12. Revised: 2024-07-23.
MR Subject Classification: 35.
Keywords: advection diffussion equation, finite difference method, diffussivity, pollution control.
Digital Object Identifier(DOI): https://doi.org/10.1007/s11766-026-5149-9.
*Corresponding author.

wide range of application including air pollutants dispersion. It is a unique tool for establishing emission control legislation, impact assessment, siting of industrial and residential complexes, emergency preparedness, planning and management etc [23]. The one dimensional ADE is formulated based on the mass conservation principle, utilizing Fick's law [4,16], offering insights into the characteristics of an unidentified function: the concentration, and contains its rate of change with respect to the location x and the time t [18]. If $C(x,t)$ is the concentration of pollutants, then the one-dimensional ADE is [13, 27]

$$\frac{\partial C}{\partial t} = D\frac{\partial^2 C}{\partial x^2} - u\frac{\partial C}{\partial x}, \tag{1}$$

where u is the velocity with which the fluid flows, also known as the mean advection velocity and D is a constant called the diffusion coefficient. The ADE (1) illustrates how the variation in concentration C relative to location affects its temporal evolution. The solution of ADE provides information about the concentration of pollutants at any time and location [8, 25].

The one-dimensional ADE continues to be an area of active research due to its applications in various scientific and engineering fields. Recent studies have focused on developing more accurate and efficient analytical and numerical methods to solve ADE and applying these solutions to practical problems such as pollutant dispersion, groundwater contamination, and heat transfer. Crank (1975) published *The Mathematics of Diffusion*, a seminal book that included extensive solutions to the one-dimensional ADE. Crank's work became a cornerstone reference for both analytical and numerical solutions to diffusion problems [7]. Schnelle et al. (2000) provided detailed descriptions of various technologies used to control and reduce air pollution, offering a thorough understanding of the principles, practices, and technologies for controlling air pollution [22]. Karahan (2008) aimed to bridge the gap between advanced numerical techniques and accessible computational tools, enhancing both learning and practical application in engineering education [15]. Goyal and Kumar (2011) focused on developing and applying mathematical models to understand and predict air pollution levels in an Indian urban environment, as well as to simulate the dispersion and concentration of air pollutants in an urban setting [11]. Ahsan (2012) aimed to demonstrate the utility of the Laplace transform finite analytical method in solving the ADE, particularly in the context of environmental and water resource management [3]. Appadu (2013) evaluated the Lax-Wendroff scheme s effectiveness by comparing it with the Crank-Nicolson scheme and a nonstandard finite difference scheme (Mickens 1991) for solving ADE with initial and boundary conditions [5]. Andallah and Khatun (2020) focused on the application of finite difference schemes to solve the ADE, involving a detailed description of the numerical methods, including the discretization process, stability analysis, and implementation details [4]. Abolfazl et al. (2021) compared FTCS, FTBSCS, BTCS, BTBSCS, and Crank-Nicholson schemes, finding the Crank-Nicholson method to closely match analytical solutions while other methods showed varying degrees of deviation [1].

Examining related research publications reveals that the authors primarily focused on comparing one-dimensional ADE solutions obtained through different numerical techniques. In contrast, this paper compares ADE solutions derived from both analytical and numerical methods. Unlike previous analytical solutions, which are based on initial conditions and cannot provide numerical pollutant concentrations at any spatial or temporal points, the analytical solution in this manuscript can numerically determine pollutant concentration at any location within the studied domain. Additionally, we investigate the relationship between diffusivity and pollutant concentration and identify the conditions under which numerical methods provide more accurate approximations for pollutant diffusivity. Furthermore, we explore how pollutant concentration changes when a pollutant with higher diffusivity enters a region of lower diffusivity, and vice versa, a scenario not addressed in prior research.

§2 Solution of advection-diffusion equation

The one-dimensional ADE for a system of length L is given by [15]

$$\frac{\partial C}{\partial t} = D\frac{\partial^2 C}{\partial x^2} - u\frac{\partial C}{\partial x} \quad (0 < x < L,\, 0 < t < \infty). \tag{2}$$

The general initial condition and the homogeneous Dirichlet boundary conditions under which the specific solution of the above model is planned to be obtained are[19]

$$C(x,0) = f(x), \tag{3}$$

$$C(0,t) = C(L,t) = 0. \tag{4}$$

To transform the ADE into a pure diffusion equation, let the nontrivial solution of (2) be given by [11]

$$C(x,t) = A(x,t)V(x,t). \tag{5}$$

The objective is to identify a function $A(x,t)$ such that the advection term in (2), i.e., uC_x, vanishes.

Plugging equation (5) into equation (2) leads to

$$V_t = DV_{xx} + \left[2D\frac{A_x}{A} - u\right]V_x + \left[-u\frac{A_x}{A} + D\frac{A_{xx}}{A} - \frac{A_t}{A}\right]V. \tag{6}$$

For the pure diffusion equation, the following conditions should hold

$$2D\frac{A_x}{A} - u = 0, \tag{7}$$

$$-u\frac{A_x}{A} + D\frac{A_{xx}}{A} - \frac{A_t}{A} = 0. \tag{8}$$

Equation (7) after integration yields

$$A = K(t)\exp\left(\frac{ux}{2D}\right), \tag{9}$$

where $K(t)$ is a constant of integration with respect to x and is a function of t only. To determine the value of $K(t)$, from the modified equation (8), we obtain

$$A_t = DA_{xx} - uA_x. \tag{10}$$

Using equation (9), we have

$$A_t = K_t\exp\left(\frac{ux}{2D}\right) = \frac{K_t A}{K}. \tag{11}$$

Using these values of A_t, A_x and A_{xx} in equation (10), assuming A as a nontrivial solution and finally integrating the result yields

$$K(t) = A_0\exp\left(-\frac{u^2}{4D}t\right), \tag{12}$$

where A_0 is a pure constant that is independent of both x and t. Using equation (12), equation (9) becomes

$$A(x,t) = A_0 \exp\left(-\frac{u^2}{4D}t\right) \exp\left(\frac{ux}{2D}\right). \tag{13}$$

Substituting the value of $A(x,t)$ from equation (13) into equation (6) and omitting all the details of algebra, we obtain

$$V_t = DV_{xx}, \tag{14}$$

which is the transformed pure diffusion equation.
The transformed initial condition is

$$V(x,0) = \exp\left(-\frac{ux}{2D}\right) f(x). \tag{15}$$

The transformed Dirichlet boundary conditions are [4]

$$V(0,t) = 0, \tag{16}$$

$$V(L,t) = 0. \tag{17}$$

Let the nontrivial solution of equation (14) be given by

$$V(x,t) = X(x)T(t). \tag{18}$$

Using equation (18), equation (14) becomes

$$XT_t = DX_{xx}T. \tag{19}$$

After rearranging the terms, we obtain

$$\frac{X_{xx}}{X} = \frac{1}{D}\frac{T_t}{T} = \lambda, \tag{20}$$

where λ is a constant. Thus, the transformed diffusion equation (14) can be split into two ordinary differential equations according to the assumption of equation (18) as

$$X_{xx} = \lambda X, \tag{21}$$

$$\frac{T_t}{T} = D\lambda. \tag{22}$$

To obtain the solution of equation (21), the corresponding boundary conditions are

$$X(0) = 0, \qquad X(L) = 0. \tag{23}$$

Depending upon the value of λ (zero, positive, or negative), three different cases arise and the non trivial solution of (21) is possible only in the case λ is negative [15]. Thus considering $\lambda = -p^2$ and using the corresponding initial and boundary conditions along with the principle of superposition, the general solution of equation (18) is the linear combination of the form [15, 21]

$$V(x,t) = \sum_{n=1}^{\infty} b_n \sin\left(\frac{n\pi x}{L}\right) \exp\left(-D\left(\frac{n\pi}{L}\right)^2 t\right), \tag{24}$$

where b_n are constants and can be calculated by using the initial condition as

$$V(x,0) = \sum_{n=1}^{\infty} b_n \sin\left(\frac{n\pi x}{L}\right) \Rightarrow \exp\left(-\frac{ux}{2D}\right) f(x) = \sum_{n=1}^{\infty} b_n \sin\left(\frac{n\pi x}{L}\right), \tag{25}$$

which is a half range Fourier Sine series and

$$b_n = \frac{2}{L}\int_0^L \exp\left(-\frac{ux}{2D}\right) f(x) \sin\left(\frac{n\pi x}{L}\right) dx. \tag{26}$$

Finally, putting together all the results obtained in equation (5), we will obtain the analytical solution to the one-dimensional advection diffusion equation as follows

$$C(x,t) = \exp\left(-\frac{u^2 t}{2D}\right)\exp\left(\frac{ux}{2D}\right)\sum_{n=1}^{\infty} b_n \sin\left(\frac{n\pi x}{L}\right)\exp\left(-D\left(\frac{n\pi}{L}\right)^2 t\right), \tag{27}$$

where b_n can be calculated by using equation (26) [6].

§3 Comparison

Consider an example of one dimensional ADE as follows

$$\begin{aligned} &\frac{\partial C}{\partial t} = D\frac{\partial^2 C}{\partial x^2} - u\frac{\partial C}{\partial x}; 0 \leq x \leq 1, t \geq 0, \\ &BCs : C(0,t) = C(1,t) = 0; t \geq 0, \\ &IC : C(x,0) = sin\pi x; 0 \leq x \leq 1. \end{aligned} \tag{28}$$

3.1 Analytical Solution

The analytical solution of the above equation is

$$C(x,t) = exp\left(-\left(\frac{u^2}{4D} + \pi^2 D\right)t\right) sin(\pi x) \tag{29}$$

Under the supposition that $u = 3.6 \times 10^{-4} m/hr$ and $D = 3.6 \times 10^{-3} m^2/hr$, the concentration of the pollutants at a distance $x = 0.6m$ from the point source at time $t = 0.6hr$ is $C(x,t) = exp(-0.03554t).sin(\pi x) = 0.93097$.

The limitation of this study is that the approach used for the analytical solution of one - dimensional ADE cannot be extended to solve two-dimensional ADE but can be utilized for one-dimensional atmospheric turbulence model. Additionally, due to the presence of negative exponent in the analytical solution, the concentration decreases over time and hence better results are achieved when the exponent of e is small and negative. After performing numerous manual calculations and rigorous analysis, we conclude that for reliable concentration measurements within the specified domain, the exponent in the analytical solution, which is independent of t, needs to be very small, i.e., to be in the order of 10^{-1} to 10^{-3} so that the magnitude of $(\frac{u^2}{4D} + \pi^2 D)t$ stays small.

3.2 Numerical Solution

In the field of numerical analysis, particularly in solving the 1D advection-diffusion equation, researchers have employed various numerical methods. Among them, three distinct approaches have been notably used: the explicit Lax-Wendroff scheme, the implicit Crank-Nicolson scheme, and a specialized nonstandard finite difference scheme as proposed by Mickens in 1991 [3]. Additionally, the explicit finite difference method has been applied to this equation. Moreover, for a comprehensive understanding and visualization of the solutions, Lazarus programming software has been utilized [20].

A key technique in simplifying the study of numerical analysis is the finite difference method. In this method, the core concept involves substituting the derivatives present in the differential equation and boundary conditions with their finite difference equivalents. This substitution leads to a linear system of equations, which can then be resolved using any conventional method [8]. Subdividing the spatial interval [0, L] into M + 1 equally spaced sample points $x_m = mh$, the time interval [0, T] into N +1 equal time points $t_n = nk$, and at each of these space-time points by introducing approximations $C(x_m, t_n) \approx V_m^n$ [10], the forward time central space scheme (FTCSS) of the one dimensional ADE is

$$V_m^{n+1} = V_m^n + \alpha[V_{m+1}^n - 2V_m^n + V_{m-1}^n] - \beta[V_{m+1}^n - V_m^n], \tag{30}$$

$$where \quad \alpha = \frac{hD}{k^2}, \quad \beta = \frac{hu}{k}.$$

Assuming length and the time intervals as $h = 0.2$ and $k = 0.2$ along with $D = 3.6 \times 10^{-3} m^2/hr$ and $u = 3.6 \times 10^{-4} m/hr$, we have $\alpha = 0.018$ and $\beta = 0.00036$.
Also,

$$V_0^n = V_M^n = 0, V_m^0 = sin(\pi mh),$$

$$\therefore V_0^0 = 0, V_1^0 = 0.5878, V_2^0 = 0.9511, V_3^0 = 0.9511, V_4^0 = 0.5878, V_5^0 = 0.$$

For $m = 1$ and $n = 0$, from equation (30), we get

$$V_1^1 = V_1^0 + \alpha[V_2^0 - 2V_1^0 + V_0^0] - \beta[V_2^0 - V_1^0] = 0.58362.$$

Table 1. Table for Numerical Results.

$V_0^0 = 0$	$V_1^0 = 0.5878$	$V_2^0 = 0.9511$	$V_3^0 = 0.9511$	$V_4^0 = 0.5878$	$V_5^0 = 0$
$V_0^1 = 0$	$V_1^1 = 0.58362$	$V_2^1 = 0.9445$	$V_3^1 = 0.9446$	$V_4^1 = 0.5841$	$V_5^1 = 0$
$V_0^2 = 0$	$V_1^2 = 0.5794$	$V_2^2 = 0.9380$	$V_3^2 = 0.9377$	$V_4^2 = 0.5802$	$V_5^2 = 0$
$V_0^3 = 0$	$V_1^3 = 0.5752$	$V_2^3 = 0.9315$	$V_3^3 = 0.9313$	$V_4^3 = 0.5764$	$V_5^3 = 0$
$V_0^4 = 0$	$V_1^4 = 0.5711$	$V_2^4 = 0.9250$	$V_3^4 = 0.9250$	$V_4^4 = 0.5726$	$V_5^4 = 0$
$V_0^5 = 0$	$V_1^5 = 0.5670$	$V_2^5 = 0.9185$	$V_3^5 = 0.9187$	$V_4^5 = 0.5688$	$V_5^5 = 0$

Table 2. Table for Analytical Results.

C(0, 0) = 0	C(0.2, 0) = 0.5878	C(0.4, 0) = 0.9511	C(0.6, 0) = 0.9511	C(0.8, 0) = 0.5878	C(1, 0) = 0
C(0, 0.2) = 0	C(0.2, 0.2) = 0.58362	C(0.4, 0.2) = 0.94432	C(0.6, 0.2) = 0.94431	C(0.8, 0.2) = 0.58361	C(1, 0.2) = 0
C(0, 0.4) = 0	C(0.2, 0.4) = 0.57948	C(0.4, 0.4) = 0.9376	C(0.6, 0.4) = 0.9376	C(0.8, 0.4) = 0.57948	C(1, 0.4) = 0
C(0, 0.6) = 0	C(0.2, 0.6) = 0.5753	C(0.4, 0.6) = 0.93099	C(0.6, 0.6) = 0.93098	C(0.8, 0.6) = 0.5753	C(1, 0.6) = 0
C(0, 0.8) = 0	C(0.2, 0.8) = 0.5713	C(0.4, 0.8) = 0.9244	C(0.6, 0.8) = 0.9243	C(0.8, 0.8) = 0.5713	C(1, 0.8) = 0
C(0, 1) = 0	C(0.2, 1) = 0.5672	C(0.4, 1) = 0.91785	C(0.6, 1) = 0.91784	C(0.8, 1) = 0.56725	C(1, 1) = 0

The figure on the left illustrates how the value of $C(x, t)$ changes as x varies between 0 and 1. It shows a trend where $C(x, t)$ initially increases from 0 to 0.94432, remains roughly constant between $x = 0.4$ and $x = 0.6$, and then decreases back to approximately 0.58361 and finally drops to 0 as x increases further.

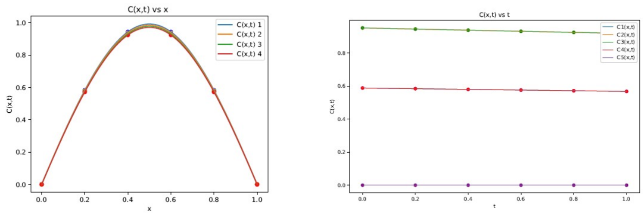

Graph of $C(x,t)$ with varying x and fixed t Graph of $C(x,t)$ with time t for various x values

Figure 1. Graphical representation.

The figure on the right illustrates how the concentration $C(x,t)$ changes over time for different fixed values of x. It shows how the initial concentrations differ and how they evolve as time progresses. Initially, each position x starts with a specific concentration value, reflecting the initial distribution of the substance or chemical. As time progresses, the concentration at each fixed position x changes, which can be observed through the lines representing different time points in the figure.

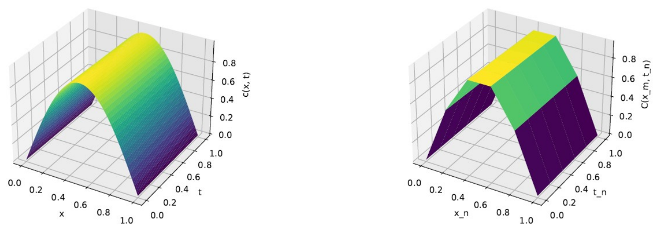

Figure 2. 3D plots for Analytical and Numerical solution of ADE.

The 3D plot in Figure 2 provides a visual representation of how the function $C(x,t)$ changes with respect to both x and t. One can observe the combined effect of exponential decay and oscillatory behavior in the resulting surface. From the mesh grid plot, we see that the function $C(x,t)$ is a product of two terms. The first term $e^{-0.03554t}$ controls the decay as t increases. As t increases, this term rapidly decreases, indicating that the function becomes smaller as t gets larger. The second term, $\sin(\pi x)$, introduces oscillations along the x-axis. The sine wave causes the surface to rise and fall as x varies. As time t increases, the oscillations decrease in magnitude, indicating that the function approaches zero for larger values of t. This visual representation helps in understanding the behavior of the function in the x, t space.

We developed the code for finite difference method. It generated a $3D$ mesh grid plot (Figure 2) to visualize the behavior of the function $C(x_m, t_n)$ over a $2D$ grid defined by spatial dimension x_m with spatial step size $h = 0.2$ and temporal dimension t_n with time step size $k = 0.2$. The color of the surface plot at each point (x_m, t_n) represents the value of $C(x_m, t_n)$ at that specific position and time. Brighter (yellow) colors indicate higher values, while darker (blue) colors indicate lower values. This concludes that 3D plot for both solutions are approximately similar and concentration of pollutants is maximum at the middle of the considered domain.

§4 Analysis of concentrations of pollutants through 3D plots

This section presents a comparison between the theoretical and computational solutions of the advection-diffusion equation. It focuses on different pollutants, specifically Ammonia - $NH_3(D = 7.92 \times 10^{-2} m^2/hr)$, Carbon monoxide - $CO(D = 7.2 \times 10^{-2} m^2/hr)$, Carbondioxide - $CO_2(D = 5.4 \times 10^{-2} m^2/hr)$ and Sulphur dioxide - $SO_2(D = 4.68 \times 10^{-2} m^2/hr)$ [12,16]. By employing the inherent diffusivity of Ammonia, Carbon Monoxide, Carbon Dioxide, and Sulphur Dioxide at a constant velocity, their respective concentrations at any given location within the domain can be determined using equation (29) as follows:

$$C(x,t) = exp\left(-\left(\frac{(3.6 \times 10^{-4})^2}{4 \times 7.92 \times 10^{-2}} + \pi^2 \times 7.92 \times 10^{-2}\right) t\right) sin(\pi x) = e^{-0.7816t} \sin \pi x,$$

$$\alpha = \frac{hD}{k^2} = \frac{0.2 \times 7.92 \times 10^{-2}}{(0.2)^2} = 0.396, \qquad \beta = \frac{hu}{k} = \frac{0.2 \times 3.6 \times 10^{-4}}{(0.2)} = 0.00036.$$

Table 3. Comparison between concentration of various pollutants.

Pollutants	Diffusivity (m^2/hr)	Velocity(m/hr)	$C(x,t)$	α	β
Ammonia (NH_3)	7.92×10^{-2}	3.6×10^{-4}	$e^{-0.7816t} sin(\pi x)$	0.396	0.00036
Carbon monoxide (CO)	7.20×10^{-2}	3.6×10^{-4}	$e^{-0.71061t} sin(\pi x)$	0.360	0.00036
Carbon dioxide (CO_2)	5.40×10^{-2}	3.6×10^{-4}	$e^{-0.53295t} sin(\pi x)$	0.270	0.00036
Sulphur dioxide (SO_2)	4.68×10^{-2}	3.6×10^{-4}	$e^{-0.4618t} sin(\pi x)$	0.234	0.00036

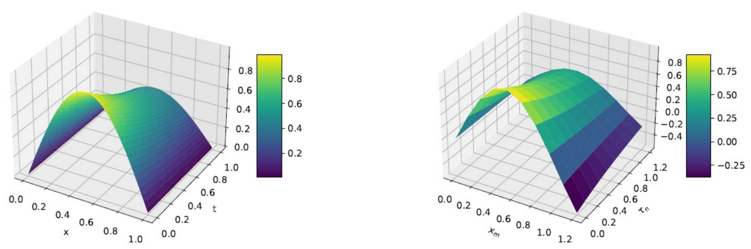

Analytical Numerical

Figure 3. $NH_3 \quad (D = 7.92 \times 10^{-2} m^2/hr)$.

The four panels of 3D graphical representations illustrate that as the diffusivity of pollutants decreases, their concentration increases. This trend holds true when other factors such as molecular size, pressure, and the nature of the medium are kept constant. Lower diffusivity means that pollutants spread out less, resulting in higher localized concentrations. The graphical representations show that with lower diffusivity, areas of high concentration become more pronounced, indicated by higher peaks in the 3D graphs. This demonstrates that pollutants remain more concentrated in specific areas when their ability to diffuse is reduced.

Analytical Numerical

Figure 4. $CO \quad (D = 7.20 \times 10^{-2} m^2/hr)$.

Analytical Numerical

Figure 5. $CO_2 \quad (D = 5.40 \times 10^{-2} m^2/hr)$.

Analytical Numerical

Figure 6. $SO_2 \quad (D = 4.68 \times 10^{-2} m^2/hr)$.

§5 Effect of diffusivity of pollutants

Dividing the spatial interval [0,1] into two equal halves and assuming the pollutants have some diffusivity enters into the region of other pollutants having different diffusivity, keeping the velocity of both the pollutants constant, the one-dimensional ADE takes the form as follows[10]

$$\frac{\partial C}{\partial t} = D_1\frac{\partial^2 C}{\partial x^2} - u\frac{\partial C}{\partial x}; \quad 0 \leq x \leq 0.5, t \geq 0, \tag{31}$$
$$\frac{\partial C}{\partial t} = D_2\frac{\partial^2 C}{\partial x^2} - u\frac{\partial C}{\partial x}; \quad 0.5 \leq x \leq 1, t \geq 0,$$

where D_1 and D_2 are the diffusivities of pollutants 1 and 2 respectively. Also let's consider

$$BCs: C(0,t) = C(1,t) = 0; t \geq 0, \tag{32}$$
$$IC: C(x,0) = sin\pi x; 0 \leq x \leq 1.$$

First, we consider pollutant 1 to be Ammonia and pollutant 2 to be Sulphur Dioxide. Subsequently, we switch the roles, considering pollutant 1 to be Sulphur Dioxide and pollutant 2 to be Ammonia. The diffusivity of Ammonia is $7.92 \times 10^{-2}\,\mathrm{m}^2/\mathrm{hr}$, while that of Sulphur Dioxide is $4.68 \times 10^{-2}\,\mathrm{m}^2/\mathrm{hr}$.

Referring to Figure 7, when the pollutant Ammonia, which has a high diffusivity, enters a region containing the pollutant Sulphur Dioxide, which has a low diffusivity, the concentration of the pollutants increases rapidly. Conversely, when the pollutant with low diffusivity, such as Sulphur Dioxide, enters a region containing the pollutant with high diffusivity, such as Ammonia, the pollutant flows forward more slowly. Consequently, the concentration of the pollutants in the region of high diffusivity increases gradually due to the slower progression of the low diffusivity pollutant.

This behavior is crucial in understanding the interaction dynamics between different pollutants in an environment. High diffusivity pollutants tend to spread more quickly and influence the surrounding area rapidly, while low diffusivity pollutants spread more slowly, leading to a more gradual change in concentration. These dynamics can significantly impact environmental modeling and pollution control strategies, as they determine how quickly pollutants disperse and interact with each other over time. Moreover, understanding these diffusivity differences helps in predicting the long-term impact of pollutant release in various ecosystems.

The plot of concentration of pollutants 'C' versus 'x' at different time levels $t = 0.5s, 1s, 1.5s$, and $2s$ with (a)Ammonia at left and Sulphur Dioxide at right (b) Sulphur Dioxide at left and Ammonia at right. In each time the maximum concentration 'C' are around $x = 0.50m$ and $x = 0.55m$ in Figure 8(a) and Figure 8(b), respectively.

Calculating the errors at different meshgrids $(0.2, 0.2)$, $(0.4, 0.6)$, $(0.6, 0.6)$, and $(0.8, 0.8)$, we can observe that the numerical solution by finite difference method for one dimensional advection diffusion equation is very close to its analytical solution and seen to be correct up to four places of decimal. The respective percentage errors are 0.0017, 0.0517, 0.0343, and 0.22. Also, pollutants having higher diffusivity has more error in numerical solution as compared to the analytical solution. Thus, numerical solution is more appropriate in case of pollutants having lower diffusivity. i.e., FTCS scheme gives better approximation for the pollutants having lower diffusivity as compared to the pollutants having higher diffusivity.

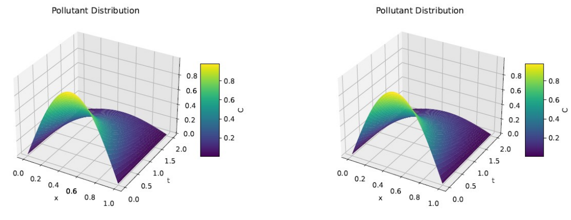

(a) (b)

Figure 7. Pollutant distribution with (a) Ammonia at left and Sulphur Dioxide at right (b) Sulphur Dioxide at left and Ammonia at right.

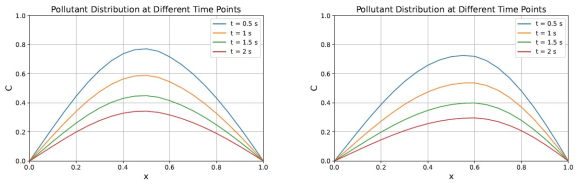

(a) (b)

Figure 8. Plot of concentration versus spatial distance at different time levels 0.5s, 1s, 1.5s and 2s with (a) Ammonia at left and Sulphur Dioxide at right (b) Sulphur Dioxide at left and Ammonia at right.

§6 Conclusion

The study presented a one-dimensional advection-diffusion equation as an illustrative example. Analytical solutions were obtained using the separation of variables method, while a numerical solution was derived through the Forward Time Central Space Scheme (FTCSS). Examining various pollutants (NH_3, CO, CO_2 and SO_2) with differing diffusivities, it was observed that pollutant concentration increases as diffusivity decreases, assuming constant influencing factors like molecular size, pressure, and medium nature. Treating the atmosphere as a non-homogeneous system, the behavior of pollutants was explored using 2D and 3D plots by equally partitioning high and low diffusivity pollutants in the domain and interchanging them. Notably, when high-diffusivity Ammonia enters the region of low-diffusivity Sulphur Dioxide, pollutant concentration rises rapidly, whereas the entry of low-diffusivity pollutants into high-diffusivity regions results in a gradual increase. Additionally, pollutants with higher diffusivity showed more numerical solution errors compared to analytical solutions, indicating that the FTCS scheme provides a better approximation for pollutants with lower diffusivity.

Our work is novel and critical for effective pollution management measures as well as environmental protection. The fundamental goal of future research is to apply turbulence to the advection diffusion model and compare the results to experimental data from the existing literature.

Declarations

Conflict of interest The authors declare no conflict of interest.

References

[1] M Abolfazl, M Mehrdad, M Ali. *Numerical solution of one-dimensional advection-diffusion equation using simultaneously temporal and spatial weighted parameters*, Australian Journal of Basic and Applied Sciences, 2011, 5(6): 1536-1543.

[2] M Ahmed, Q U A Zainab, S Qamar. *Analysis of one-dimensional advection-diffusion model with variable coefficients describing solute transport in a porous medium*, Transport in Porous Media, 2017, 118: 327-344.

[3] M Ahsan. *Numerical solution of the advection-diffusion equation using Laplace transform finite analytical method*, International Journal of River Basin Management, 2012, 10(2): 177-188.

[4] L S Andallah, M R Khatun. *Numerical solution of advection-diffusion equation using finite difference schemes*, Bangladesh Journal of Scientific and Industrial Research, 2020, 55(1): 15-22.

[5] A R Appadu. *Numerical Solution of the 1D Advection-Diffusion Equation Using Standard and Nonstandard Finite Difference Schemes*, Journal of Applied Mathematics, 2013, 2013(1): 734374.

[6] V Aswin, A Awasthi, C Anu. *A comparative study of numerical schemes for convection-diffusion equation*, Procedia Engineering, 2015, 127: 621-627.

[7] J Crank. *The mathematics of diffusion*, Oxford: Oxford University Press, 1975.

[8] K S M Essa, S M Etman, M S El-Otaify. *Modeling of atmospheric dispersion with dry deposition: an application on a research reactor*, Revista Brasileira de Meteorologia, 2014, 29(3): 331-337.

[9] S J Farlow. *Partial differential equations for scientists and engineers*, Courier Corporation, 1993.

[10] M B Glinowiecka-Cox. *Analytic solution of 1d diffusion-convection equation with varying boundary conditions*, University Honors Theses, 2022, DOI: 10.15760/honors.1224.

[11] P Goyal, A Kumar. *Mathematical modeling of air pollutants: An application to Indian urban city*, Air Quality-Models and Applications, 2011, 101-130.

[12] B Grewal, J Grewal. *Numerical Methods in Engineering & Science: With Programs in C, C++ & MATLAB*, Khanna, 2014.

[13] D K Jaiswal, A Kumar, R R Yadav. *Analytical Solution to the One-Dimensional Advection-Diffusion Equation with Temporally Dependent Coefficients*, Journal of Water Resource and Protection, 2011, 3(1): 76-84.

[14] J Kafle, L P Bagale, D J KC. *Numerical solution of parabolic partial differential equation by using finite difference method*, Journal of Nepal Physical Society, 2020, 6(2): 57-65.

[15] H Karahan. *Solution of weighted finite difference techniques with the advection-diffusion equation using spreadsheets*, Computer Applications in Engineering Education, 2008, 16(2): 147-156.

[16] A Kumar, D K Jaiswal, N Kumar. *Analytical solutions of one-dimensional advection-diffusion equation with variable coefficients in a finite domain*, Journal of Earth System Science, 2009, 118: 539-549.

[17] J J McKetta. *Chemical engineers handbook*, New York: The McGraw-Hill Companies, Inc., 1963.

[18] G Parker. *Encyclopedia of materials: science and technology*, Oxford: Elsevier, 2001.

[19] M L Brusseau, I L Pepper, C P Gerba. *Environmental and pollution science*, Academic Press, 2019.

[20] K S Rao. *Introduction to partial differential equations*, PHI Learning Pvt. Ltd., 2010.

[21] R C Reid, J M Prausnitz, T K Sherwood. *The properties of gases and liquids (3rd ed.)*, McGraw-Hill Chemical Engineering Series, 1977, 629-665.

[22] B K Schnelle Jr, C A Brown. *Air pollution control technology handbook*, Boca Raton: CRC press, 2016.

[23] M Sharan, M Modani. *A two-dimensional analytical model for the dispersion of air-pollutants in the atmosphere with a capping inversion*, Atmospheric Environment, 2006, 40(19): 3479-3489

[24] J M Stockie. *The mathematics of atmospheric dispersion modeling*, Siam Review, 2011, 53: 349-372.

[25] W A Strauss. *Partial differential equations: An introduction*, Hoboken: John Wiley & Sons, Inc., 2007.

[26] S Ulfah, S A Awalludin, Wahidin. *Advection-diffusion model for the simulation of air pollution distribution from a point source emission*, Journal of Physics: Conference Series, 2018, 948: 012067.

[27] C Zoppou, J Knight. *Analytical solutions for advection and advection-diffusion equations with spatially variable coefficients*, Journal of Hydraulic Engineering, 1997, 123: 144-148.

[1]Institute of Science and Technology, Tribhuvan University, Tri-Chandra Multiple Campus, Nepal.
Email: eeshwarpoudel475@gmail.com

[2]Department of Applied Mathematics, University of Alabama at Birmingham, AL, USA.
Email: pacharya@uab.edu

[3]Institute of Science and Technology, Central Department of Mathematics, Tribhuvan University, Nepal.
Emails: jeevan.kafle@cdmath.tu.edu.np, shreeramkhadka@gmail.com